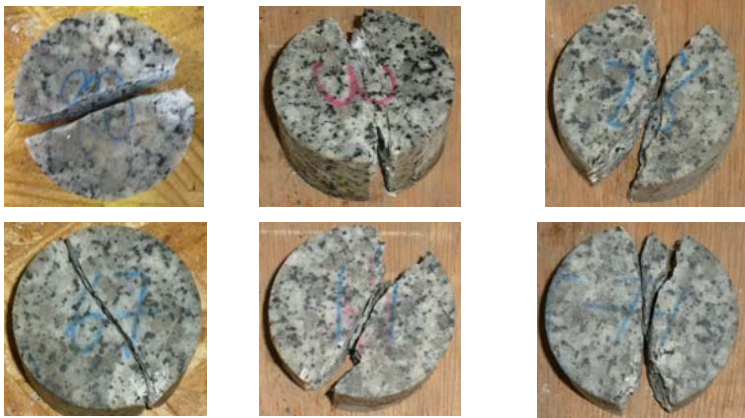


Brazilian Splitting tests for granite

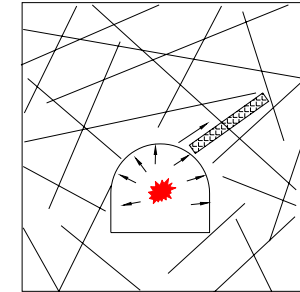


Quasi-static load With lower dynamic load With higher dynamic load

Rock Joint Dynamic Properties



Joins in rock mass



Stress wave propagation
in rock mass

Stress Wave Propagation in Rock Mass

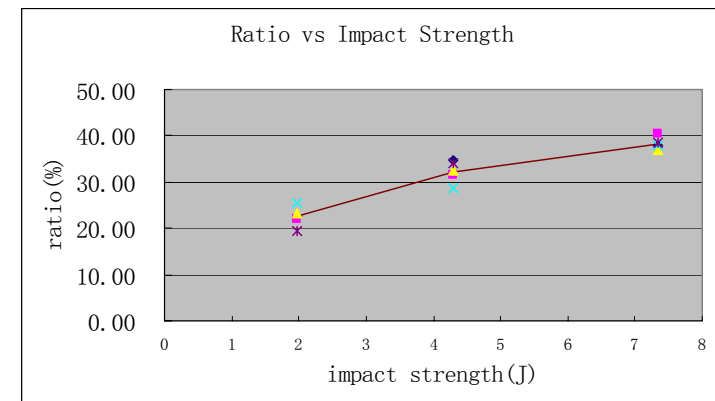


- Two granite pressure bars
- A discontinuous layer between the pressure bars
- Aperture and water content effects

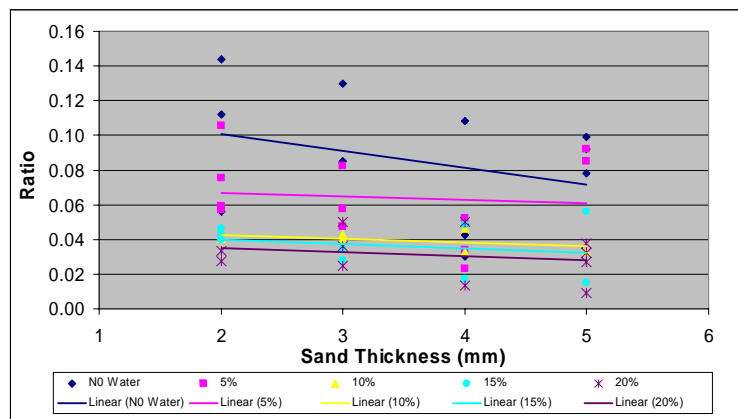


- Multiple joint layers

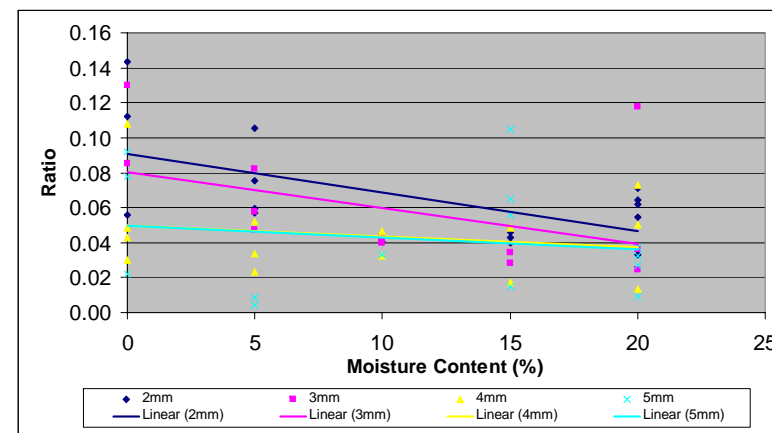
Impact Energy Effect



Aperture effects

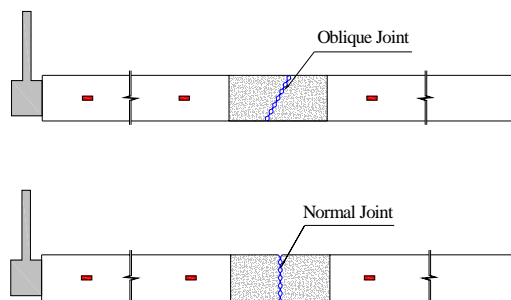


Effect of Water Content

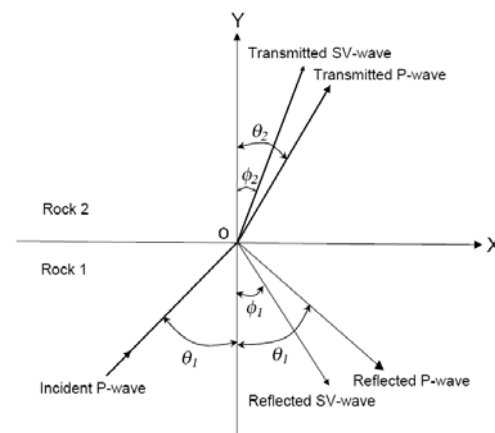


SHPB tests for oblique joint

- Effect of joint orientation on wave transmission and reflection



Wave Propagation Across Single Joint



$$\sigma_{yy}^- = \sigma_{yy}^+$$

$$\tau_{xy}^- = \tau_{xy}^+$$

$$\Delta v = v^- - v^+ = \frac{\sigma_{yy}}{k_n}$$

$$\Delta u = u^- - u^+ = \frac{\sigma_{xy}}{k_\tau}$$

2-D P-wave propagation Displacement discontinuity theory

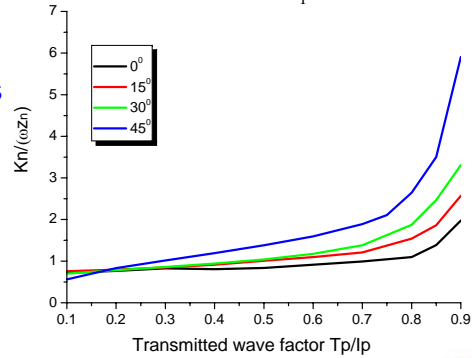
Different Joint Orientation Cases

incident p-wave

$$w_{lp} = -Ie^{-i\omega t} \left\{ \cos \theta_1 \cdot \exp\left[\left(\frac{i\omega}{\alpha_1}\right) \cdot (x \sin \theta_1 - z \cos \theta_1)\right] \right\}$$

$$u_{lp} = Ie^{-i\omega t} \left\{ \sin \theta_1 \cdot \exp\left[\left(\frac{i\omega}{\alpha_1}\right) \cdot (x \sin \theta_1 - z \cos \theta_1)\right] \right\}$$

Normal stiffness



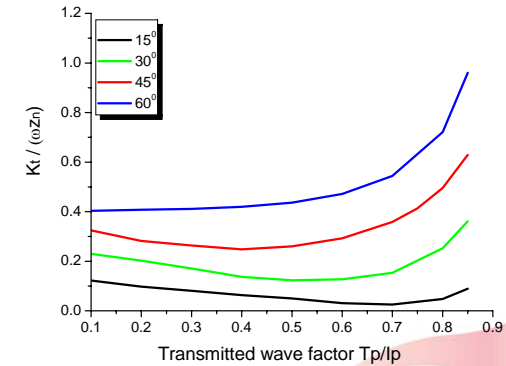
Different Joint Orientation Cases

incident p-wave

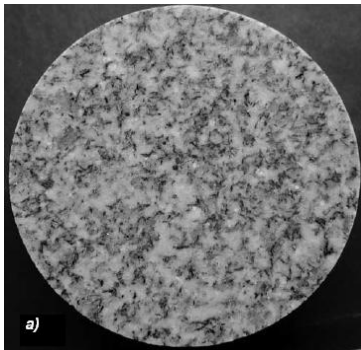
$$w_{lp} = -Ie^{-i\omega t} \left\{ \cos \theta_1 \cdot \exp\left[\left(\frac{i\omega}{\alpha_1}\right) \cdot (x \sin \theta_1 - z \cos \theta_1)\right] \right\}$$

$$u_{lp} = Ie^{-i\omega t} \left\{ \sin \theta_1 \cdot \exp\left[\left(\frac{i\omega}{\alpha_1}\right) \cdot (x \sin \theta_1 - z \cos \theta_1)\right] \right\}$$

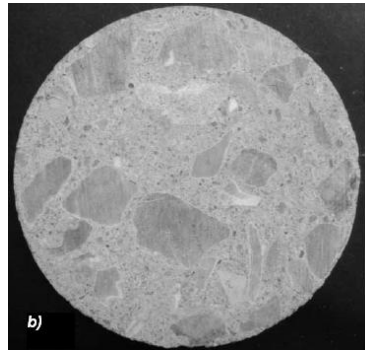
Tangent stiffness



Modeling Heterogeneity Effect



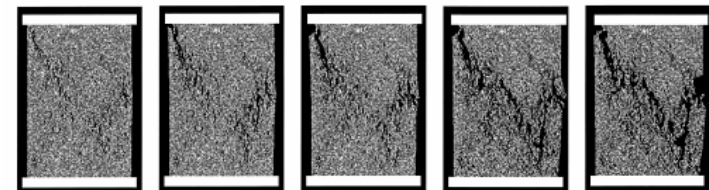
Granite sample



Concrete sample

Modeling Material Heterogeneity

- Weibull Distribution
 - Statistical method
 - Describes the microstructures well
 - Adopted in numerical simulations in FEM
 - Rock Failure Process Analysis (RFPA), Tang et al. (2000)



Simulations on rock failure under compression considering material heterogeneity by Tang et al. (2000)

SPH Method

- Approximations of SPH
 - Kernel (smoothing) Function
 - Delta function property
 - Normalization
 - Compactly supported
 - Smoothing property
 - Kernel approximation

Illustration of one kernel function in 1-D

Supporting domain

$$f(x) = \int f(x') W(x-x', h) dx'$$

$$\nabla f(x) = \int f(x') \nabla W(x-x', h) dx'$$

- Particle approximation

$$f_i = \sum_{j=1}^N \left(\frac{m_j}{\rho_j} \right) f_j W(x_i - x_j, h)$$

$$\nabla f_i = \sum_{j=1}^N \left(\frac{m_j}{\rho_j} \right) f_j \nabla W(x_i - x_j, h)$$

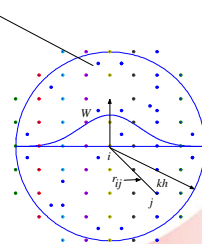
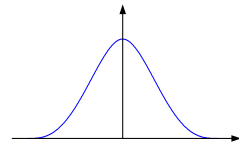


Illustration of SPH approximations

SPH Method

- Governing equations & SPH approximations

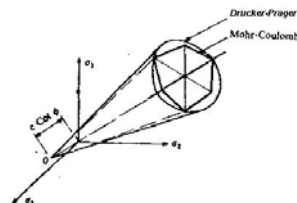
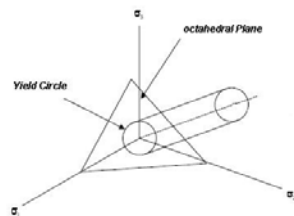
$$\begin{cases} \frac{d\rho}{dt} = -\rho \cdot \frac{\partial v^\alpha}{\partial x^\alpha} \\ \frac{dv^\alpha}{dt} = -\frac{1}{\rho} \cdot \frac{\partial \sigma^{\alpha\beta}}{\partial x^\beta} \\ \frac{de}{dt} = -\frac{\sigma^{\alpha\beta}}{\rho} \cdot \frac{\partial v^\alpha}{\partial x^\beta} \end{cases}$$



$$\begin{cases} \frac{d\rho_i}{dt} = \rho_i \sum_{j=1}^N \frac{m_j}{\rho_j} v_{ij}^\alpha \frac{\partial W_{ij}}{\partial x_i^\alpha}; \quad \rho_i = \sum_{j=1}^N m_j W_{ij} \\ \frac{dv_i^\alpha}{dt} = -\sum_{j=1}^N m_j \left(\frac{\sigma_i^{\alpha\beta}}{\rho_i^2} + \frac{\sigma_j^{\alpha\beta}}{\rho_j^2} \right) \frac{\partial W_{ij}}{\partial x_i^\beta} \\ \frac{de_i}{dt} = \frac{1}{2} \sum_{j=1}^N m_j v_{ij}^\beta \left(\frac{\sigma_i^{\alpha\beta}}{\rho_i^2} + \frac{\sigma_j^{\alpha\beta}}{\rho_j^2} \right) \frac{\partial W_{ij}}{\partial x_i^\beta} \end{cases}$$

SPH Method

- Constitutive model
 - Elasto-plastic constitutive model
 - Failure criterions
 - von Mises yield criterion
 - Mohr-Coulomb criterion



Geometrical representation of the von Mises (left) and Mohr-Coulomb (right) yield surfaces in principal stress space

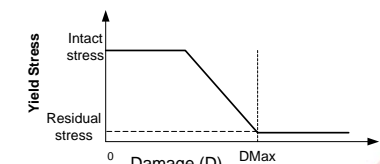
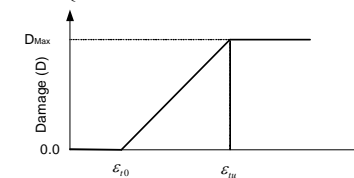
SPH Method

- Isotropic tensile damage model

$$D = \begin{cases} 0 & , \varepsilon_t < \varepsilon_{t0} \\ D_{Max} \left(\frac{\varepsilon_t - \varepsilon_{t0}}{\varepsilon_{tu} - \varepsilon_{t0}} \right) & , \varepsilon_{t0} \leq \varepsilon_t < \varepsilon_{tu} \\ D_{Max} & , \varepsilon_t \geq \varepsilon_{tu} \end{cases}$$

$$\varepsilon_{t0} = \frac{f_{t0}}{E_0}$$

$$\varepsilon_{tu} = \lambda_u \varepsilon_{t0}$$



Isotropic tensile damage model (left); Illustration for the yield stress degraded with the damage (right) in uniaxial stress state

Modeling Material Heterogeneity

- Weibull distribution equation

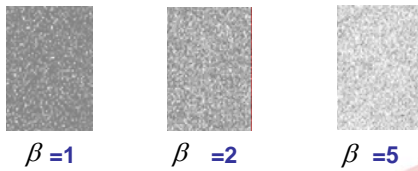
$$f(T) = \frac{\beta}{\mu} \left(\frac{T}{\mu} \right)^{\beta-1} e^{-\left(\frac{T}{\mu} \right)^{\beta}}; T \geq 0, \mu > 0, \beta > 0$$

μ : seed parameter, β : homogenous index

- Implementation



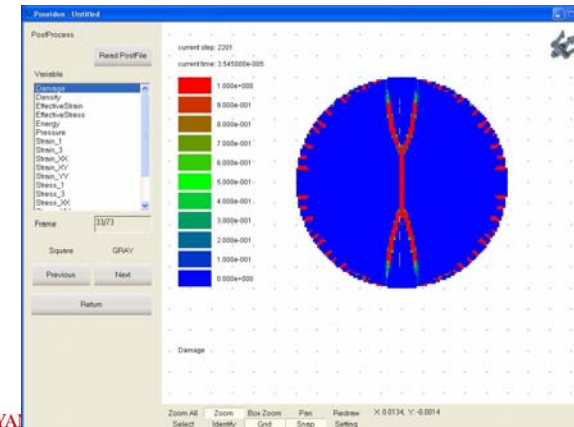
- Numerical specimens



Distributions by different heterogeneous indices

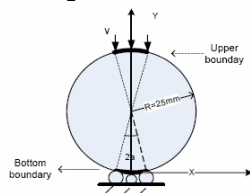
Program Implementation & Calibration

- Program Implementation with pre-processor & post-processor

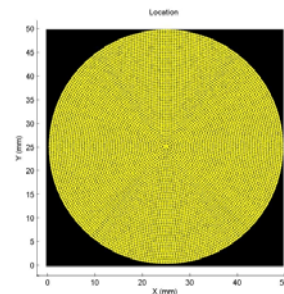


Simulations on Brazilian Splitting Test

- Numerical Model Configuration
 - Elasto-plastic model with M-C criterion
 - Isotropic tensile damage model
 - Tensile strength as a critical parameter to investigate heterogeneous effects



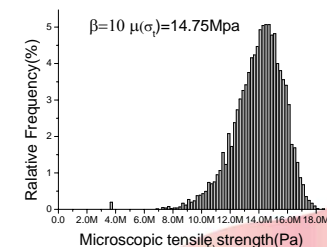
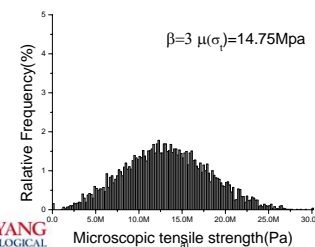
Geometry and loading condition for disc specimen under the dynamic load (R=25mm, $\alpha=6.9^\circ$)



Simulations on Brazilian Splitting Test

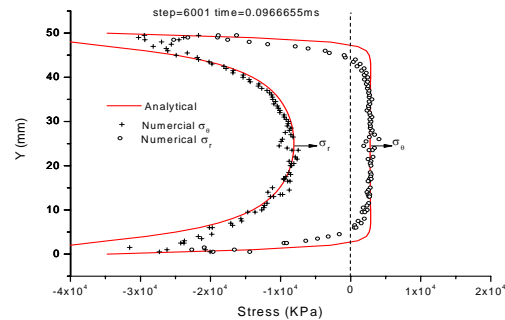
- Cases Under Low Loading Rate ($v=-0.1\text{m/s}$)
 - Heterogeneity model setting

Case No.	σ_{th} (MPa)	ρ, ν, E, c, ϕ
	β	$\mu(\sigma_{th})$
1	3	14.75
2	10	14.75



Simulations on Brazilian Splitting Test

- Cases Under Low Loading Rate ($v=-0.1\text{m/s}$)



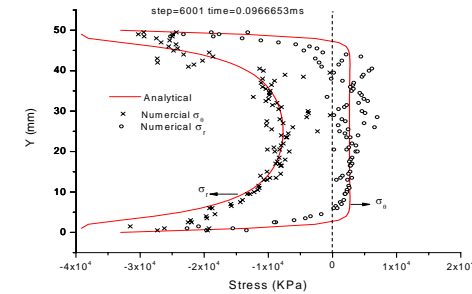
Analytical and simulated stress distributions along the loading axis

Case 2 $\beta=10$



Simulations on Brazilian Splitting Test

- Cases Under Low Loading Rate ($v=-0.1\text{m/s}$)



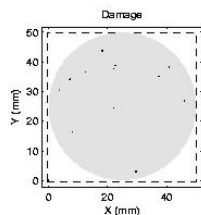
Analytical and simulated stress distributions along the loading axis

Case 1 $\beta=3$

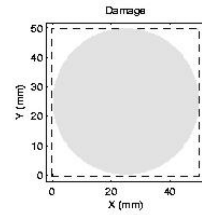


Simulations on Brazilian Splitting Test

- Cases Under Lower Loading Rates



Case 1 $\beta=3$



Case 2 $\beta=10$

Variations of damage distribution during the fracture process

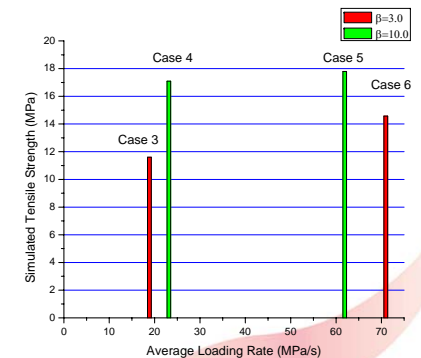


Simulations on Brazilian Splitting Test

- Cases Under Higher Loading Rates
 - Loading rates and simulated tensile strengths
 - Simulated tensile strength

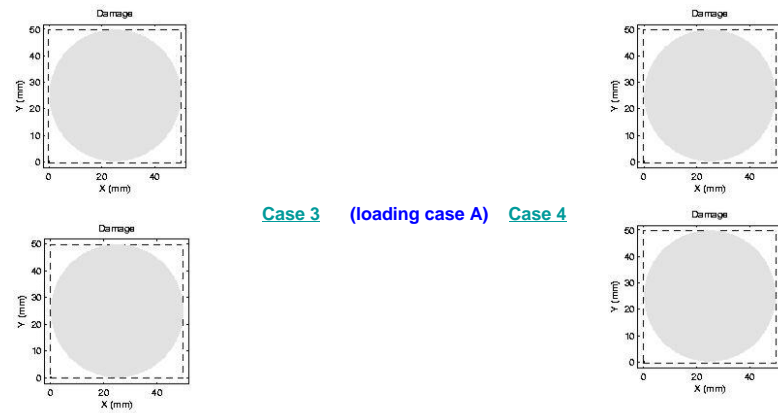
$$\sigma_x \approx -\frac{P}{\pi RL}$$

- Strength gets increased with the Loading Rate
- Improvement was affected by the material heterogeneity



Simulations on Brazilian Splitting Test

- Cases Under High Loading Rates (Fracture processes)



Variations of damage distribution during the fracture process

Simulations on Brazilian Splitting Test

- Cases Under High Loading Rates (Final Fracture patterns)

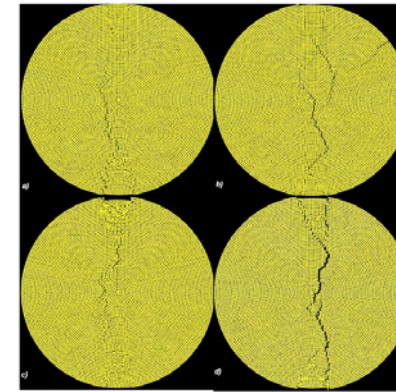
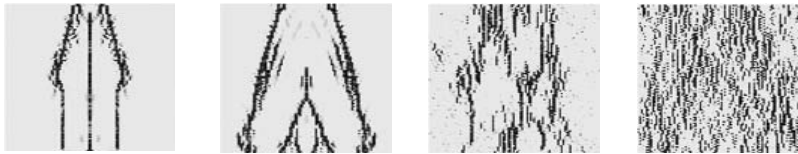
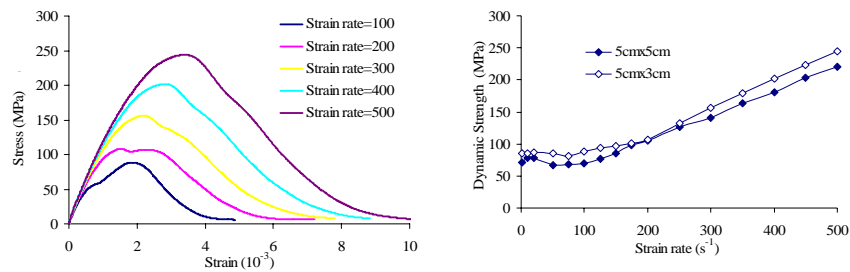


Figure 5-24 Cracks simulated in Case 3, 4, 5 and 6, from a) to d).



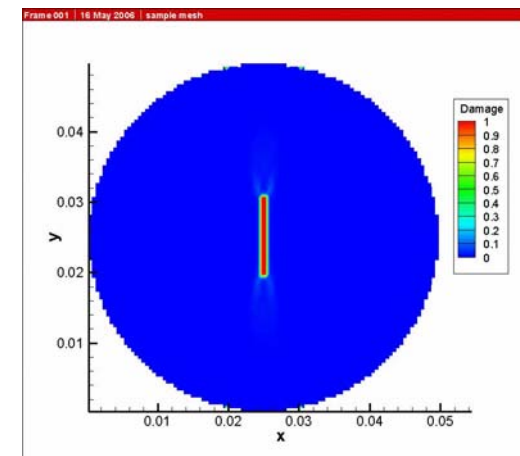
Strain Rate Effect



Strain rate increase

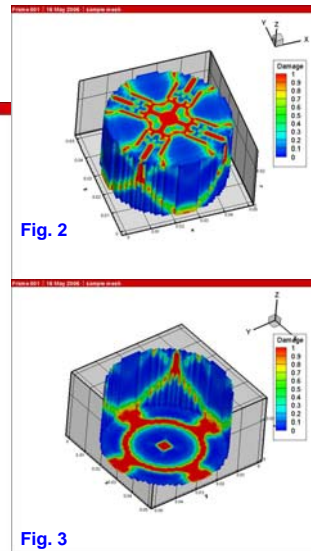
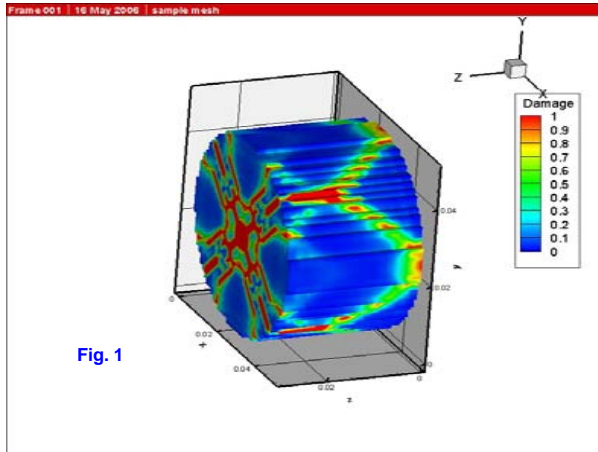


Ongoing Works – Advanced Constitutive Model



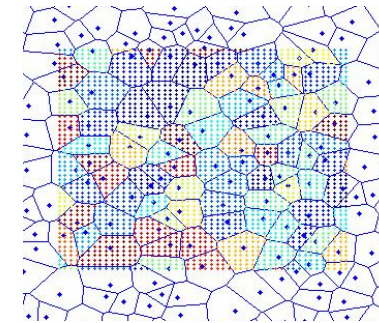
Ongoing Works – 3D Model

- Rock splitting simulations in 3-D

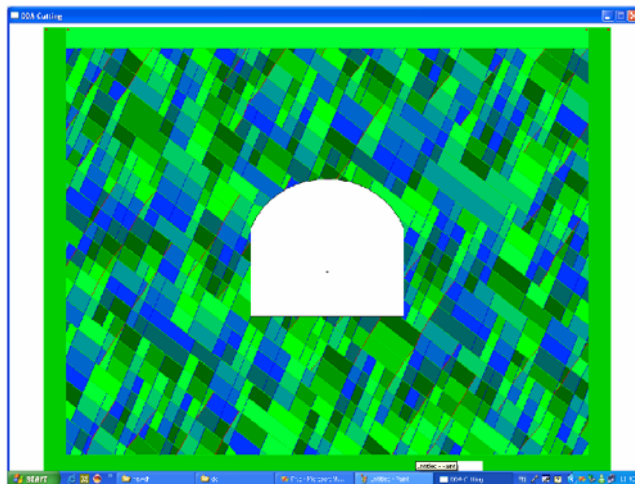


Ongoing work – Generalized SPH Method

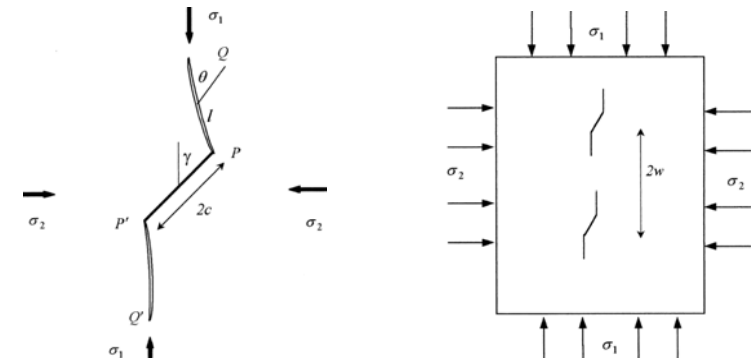
- Considering material heterogeneity
 - Using Voronoi polygons
 - Aggregates, composites
 - Rock joints, discontinuum



Ongoing Work – Application of Manifold Method

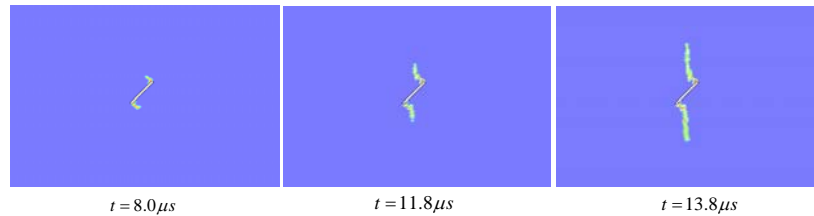


The Role of Fracture Mechanics –Sliding Crack Model



Wing-crack model and simplified model for array
preexisting crack

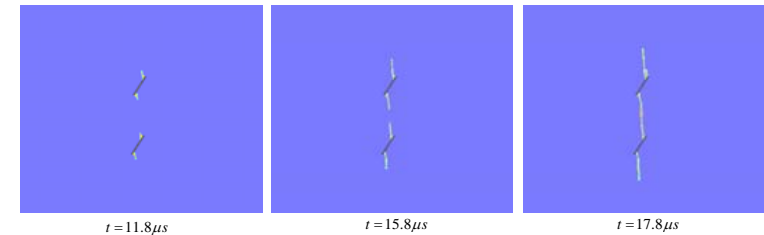
The Role of Fracture Mechanics –Sliding Crack Model



45°, $v=0.5\text{m/s}$, length of preexisting crack=1.0cm

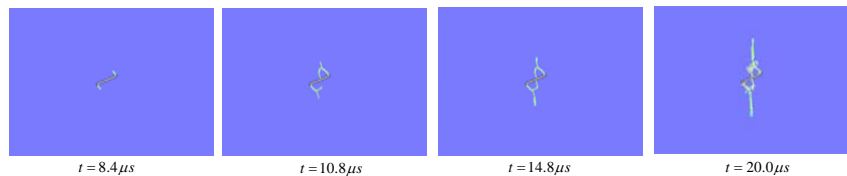
The Role of Fracture Mechanics –Sliding Crack Model

Effect of different orientation and strain rate on crack growth

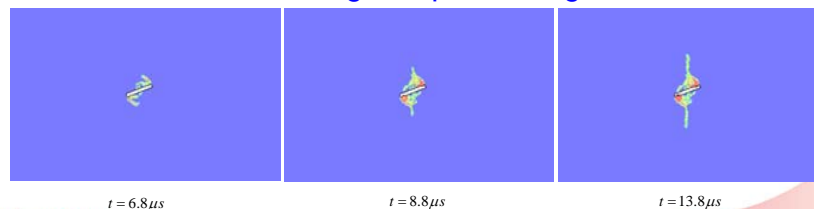


60°, $v=1.0\text{m/s}$, same preexisting cracks=1.0cm

The Role of Fracture Mechanics –Sliding Crack Model

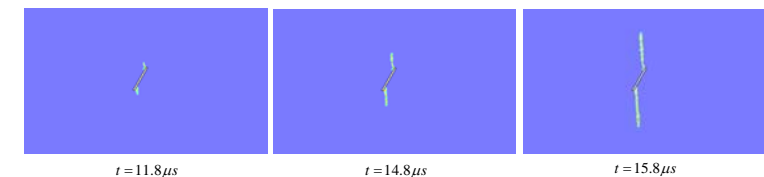


20°, $v=0.1\text{m/s}$, length of preexisting crack=1.0cm

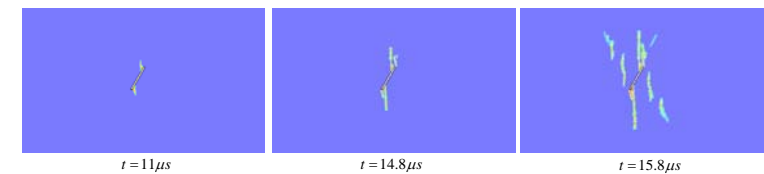


20°, $v=0.5\text{m/s}$, length of preexisting crack=1.0cm

The Role of Fracture Mechanics –Sliding Crack Model

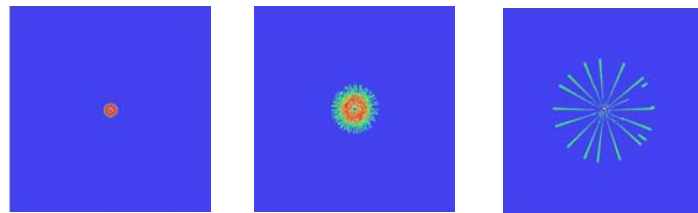


60°, $v=0.5\text{m/s}$, length of preexisting crack=1.0cm



60°, $v=1.5\text{m/s}$, length of preexisting crack=1.0cm

Borehole Blast Simulation: Influence of Loading Rate



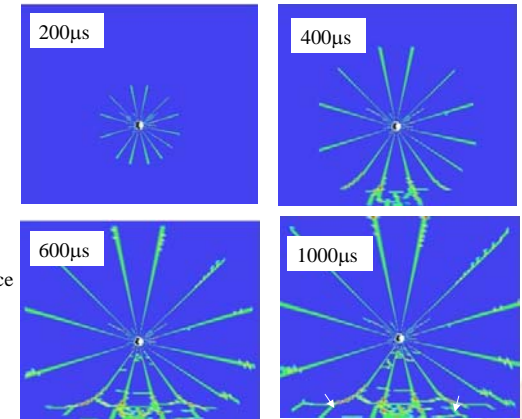
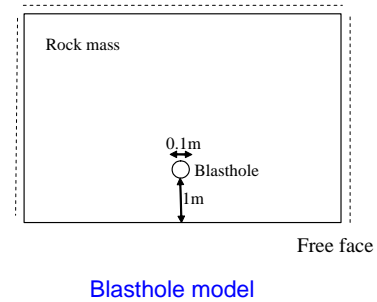
(a) 20 MPa/μs

(b) 10 MPa/μs

(c) 1.0 MPa/μs

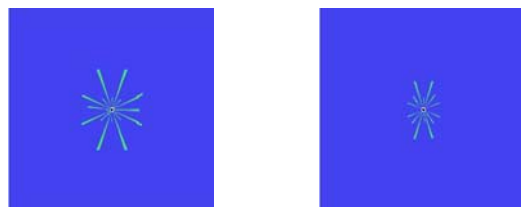
Fracture pattern under different loading rate

Borehole Blast Simulation



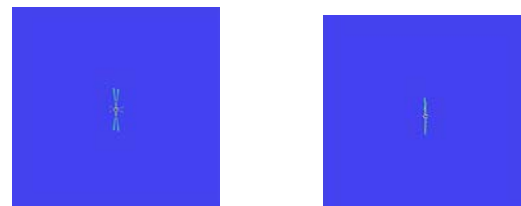
Fracture Process

Influence of Pre-existing Stress



(a) 2 MPa

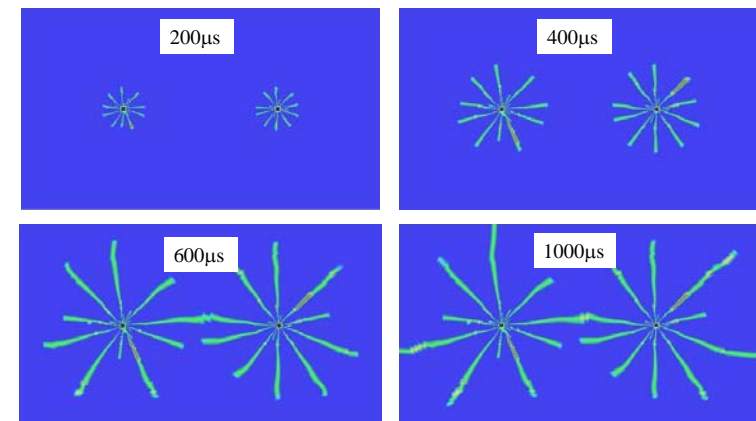
(b) 10 MPa



(c) 30 MPa

(d) 50 MPa

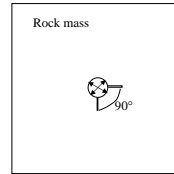
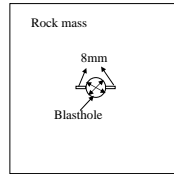
Crack Connections



Effectiveness of Blast damage control

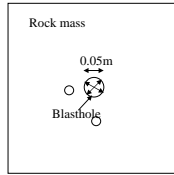
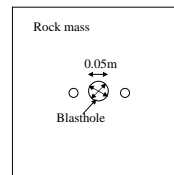
Control I

Blasthole with notches



Control II

Blasthole with concurrent holes



Control III



Charge holder with slits

Summary

- Rock and rock joint dynamic properties.
- Mechanism of strain rate effect on rock dynamic failure.
- Modeling heterogeneity effect.
- Fracture mechanics versus damage mechanics.
- Continuum model versus discontinuous model.
- Rock engineering applications.

Thank you !